The Novel Application of Asphalt in Cross-Linked Polyethylene Composite

Yi Liao
State Key Laboratory of Polymer Materials Engineering,polymer research institute of Sichuan university
Shuangxin Lai
State Key Laboratory of Polymer Materials Engineering,polymer research institute of Sichuan university
Shuangqiao Yang
State Key Laboratory of Polymer Materials Engineering,polymer research institute of Sichuan university
Jinjing Liu
state key laboratory of special functional waterproof materials
shibing bai (baishibing@scu.edu.cn)
State Key Laboratory of Polymer Materials Engineering,Polymer Research Institute of Sichuan Universiry
https://orcid.org/0000-0001-8798-8768

Research Article

Keywords: waste cross-linked polyethylene (XLPE) cables, asphalt, solid-state shear milling, modification, thermoplastic processing properties

Posted Date: May 11th, 2021

DOI: https://doi.org/10.21203/rs.3.rs-482238/v1

Abstract

The cross-linked polyethylene (XLPE) cables are widely used as an important basic material for power transportation. However, the cross-linked network structure caused challenge in the recycling of waste XLPE, which usually be treated by incineration and landfilling. In this research, XLPE was de-crosslinked via solid-state shear milling (S^3M) and the asphalt was used as plasticizer during the thermoplastic processing. To deeply understand the influence of asphalt on the matrix, the compatibility, dispersion, and rheological properties of composites were characterized. Due to the good compatibility between de-crosslinked XLPE and asphalt, the viscosity of the composites decreased significantly. Some sea-island structure also formed in composites, which increased the toughness of the composites and the elongation at break reach as high as 322%. The use of asphalt to achieve the processing performance of de-crosslinked XLPE powder was highly effective and composites can be processed by ordinary polymer processing equipment. Furthermore, the prepared composites show potential application in the field of waterproofing which could recycle of waste XLPE cables in large-scale.

1. Introduction

For cross-linked polyethylene (XLPE), the van der Waals forces between polyethylene molecules are replaced by chemical bonds[1], which form a three-dimensional network structure and making it difficult for the molecules to slip. This network structure effectively improves the mechanical properties, heat resistance, environmental stress cracking resistance, and chemical resistance[2]. The XLPE has a wide range of applications such as cables, conveying pipes, and heat-shrinkable products[3]. The peroxide cross-linking, irradiation cross-linking, and silane cross-linking are three main kinds of cross-linking methods in the industry. The first two of crosslinking methods used initiators to achieve cross-linking purposes, and the last one uses physical methods[4–6]. With the large-scale upgrade of communication and power grid facilities, a large amount of XLPE cable scrap was generated. But as an insoluble and infusible thermosetting material, how to recycle XLPE cables has always been a serious problem. Conventional direct incineration and landfill caused the leakage of waste liquid, the emission of waste gas, and pollute the land[7, 8]. They are not in line with the current concept of sustainable green development[9]. However, the green, high-quality, and efficient recycling of XLPE waste is still a huge challenge.

According to literature, the recycling methods of XLPE include thermal shear plasticization recycling[10], powdered filler recycling, supercritical fluid recycling, and ultrasonic-assisted recycling[11–13]. Above technology faced with defects of poor mechanical properties of materials, large equipment investment and strict process requirements[14–16]. Based on the pursuit of simpler and more efficient XLPE recycling technology, a self-developed solid-state shear milling (S^3M) technology was used to recycle the material[17–20]. S^3M equipment is based on traditional Chinese stone pan mill, which not only can crush and mix, but also act as a mechanochemical reactor. With the unique three-dimensional shear structure, the materials in the equipment are subjected to shearing, squeezing, and stretching stress fields. The motion trajectory of material is a spiral line, which has a long path enables the equipment to realize the

functions of crushing, dispersing, mixing, etc[17]. This technology has been reported to destroy the cross-linked bond of silane cross-linked polyethylene (Si-XLPE) and achieved the fracture between some -C-Si- and -O-Si-O- bonds[21], resulting in thermoplastic processable polyethylene. To further realize the value-added application of XLPE powder, it is important to improve the processing performance of composites.

Asphalt is the residue of coking or crude oil distillation and it is mainly composed of alkane compounds composed of carbon and hydrogen[22]. Due to the characteristics of waterproof, moisture-proof, and corrosion-proof, asphalt is often used in the field of waterproofing and paving roads. Nowadays, bituminous waterproofing membrane modified by rubber powder integrated bonding, sealing, and waterproofing and has gradually replaced the traditional waterproofing membrane [23–25]. Due to the presence of small relative molecular weight alkanes, the asphalt not only has good thermoplastic fluidity but also has good compatibility with polyethylene.

This study shown the novel application of asphalt in waste peroxide cross-linked polyethylene (WP-XLPE) composite. In the first step, WP-XLPE powder was prepared by S^3M technology. Through the strong shear force, the cross-linked structures of WP-XLPE materials were destroyed. Then, asphalt added as a plasticizer to give the powder excellent processing performance. From the results of SEM and DMA, it can be obtained that the asphalt and WP-XLPE have good compatibility and uniform dispersion. The rheological test shows that the addition of asphalt greatly improved the ability of processing in WP-XLPE thermoplastic extrusion. The composite sheets can be successfully extruded by a screw. It is expected that such a sheet has potential to be used as waterproof material.

2. Experimental Protocols

2.1 Materials

The waste peroxide cross-linked polyethylene cable mainly includes three parts: conductor shielding layer, insulating layer, and insulating shielding layer, provided by TBEA Deyang Cable Co., Ltd. (Sichuan China), which consisted of 75% P-XLPE and 25% EVA.

90# asphalt: the label is determined by the penetration degree, and its basic performance is shown in Table. 1, provided by Beijing Oriental Yuhong Co., Ltd.

Table 1
Basic properties of asphalt matrix

Asphalt	90
Needle penetration/25 ℃ (0.1mm)	80 ~ 90
Ductility/10 ℃ (cm)	> 20
Softening point (℃)	42 ~ 49
Wax content (%)	< 2.6
Solubility (%)	> 99.9

2.2 Preparation of asphalt/WP-XLPE composites

The preparation scheme of asphalt/WP-XLPE composites is shown in Figure.1. The WP-XLPE cable was crushed into 2–3 cm particles by plastic crusher and then fed into the solid-state shear milling (S^3M) equipment to prepare the WP-XLPE powder with 10 milling cycles of 50 rpm. In this milling process, the temperature is controlled by the cooling water. This instrument used the relative movement between two milling pans with grooves and ridges to produce a huge shearing force and make the material spiral outward from the center of the pan at a rotation speed.

The WP-XLPE powder was mixed with asphalt of different mass ratios through an internal mixer at a speed of 50rpm and under the temperature of 180℃. 10 minutes later, the material was taken out and crushed. Then the composite material fragments were made into sheets in two ways: the first one, under 180 ℃ and 10MPa, hot pressing for ten minutes, then cold pressing under the same pressure for 10 minutes; the second one, extruding with a screw extruder, the temperatures of barrels were 150℃, 175℃, 180℃, 175℃ and the screw was maintained at a speed of 100 rpm.

2.3 Characterization

2.3.1 Fourier Transform Infrared Spectroscopy (FT-IR)

A Nicolet 6700 FT-IR spectrometer was utilized to acquire the molecule structure and functional groups of the samples. The spectra were recorded from 4,000 cm^{-1} to 400 cm^{-1} at a resolution of 4 cm^{-1} over 32 scans.

2.3.2 X-ray Photoelectron Spectroscopy (XPS)

An X-ray photoelectron spectrometer was used to identify all the elements present in the composite material through an accelerating voltage of 15 kV and an emission current of 10 mA.

2.3.3 Dynamic Mechanical Analysis (DMA)

A DMA of TA instruments (model Q850) in three-point bending mode was utilized to study the dynamic mechanical properties of specimens. Dynamic loss (tan δ) was determined at a frequency of 1 Hz and a

heating rate of 3℃*min^{-1}as a function of temperature in the range of -100℃ to 100℃.

2.3.4 Scanning Electron Microscope (SEM)

All asphalt/WP-XLPE composites of different components were brittle fractured in liquid nitrogen and then immersed in n-hexane to etch away the asphalt. Observed the morphology of the cross-section with an Inspect (FEI) scanning electron microscopy instrument to analyze the polymer morphology and the distribution of asphalt in the matrix. All samples were sputter-coated with gold.

2.3.5 Differential Scanning Calorimetry (DSC)

Using the TA Q20 differential scanning calorimeter to test the melting and crystallization behavior of composite samples, with nitrogen atmosphere protection to prevent the change of asphalt composition. Recorded the DSC curve, with the temperature range of -70°C to 200°C, at a heating rate of 10°C* min^{-1}. In this temperature range, the sample has undergone a process from heating to cooling

2.3.6 Thermogravimetric Analysis (TGA)

The TGA-Q50 from TA Instruments was used to study the thermal stability of composite asphalt materials, using a heating rate of 10°C* min^{-1} in nitrogen atmosphere from 25°C to 700°C.

2.3.7 High-Pressure Capillary Rheometer

The high-pressure capillary rheological analysis was utilized to test the shear flow behavior of different composition materials. The experimental parameters were set as follows: L/D = 20/2,180°C, shear rate range of 50 ~ 1500 s^{-1}.

2.3.8 Torque Rheometer

The torque rheometer was utilized to test the torque rheological properties of materials with different compositions. About 50g of the sample was added to the rheometer to melt and mix at 180°C, and the motor speed was set at 50rpm/min for 10min. During the experiment, the torque curve was recorded by the computer.

2.3.9 Mechanical Properties

The universal tensile testing machine was utilized to test tensile strength and elongation at break. The experimental samples were subjected to conventional tensile tests according to the test standard ASTM D412, with a tensile speed of 50 mm/min.

3. Results And Discussion

3.1 Changes in chemical bonds and groups of materials

To explore the relationship between the compatibility of the two in the composite material and the chemical structure, the rubber powder, asphalt, and composite materials were characterized by FTIR. The

analysis results of WP-XLPE with different milling cycles in Figure.2(a) show that they all have common characteristic bands: there are three strong absorption peaks at 2920cm^{-1}, 1470cm^{-1}, and 722cm^{-1}, which belong to the expansion, bending, and swing vibrations of C-H, all of which are the infrared characteristic absorption peaks of polyethylene. And 722cm^{-1} belongs to the absorption peak of amorphous PE[7], indicating that the WP-XLPE after S3M treatment has a de-crosslinked part. It is worth noting that as the number of milling cycles increases, there are obvious characteristic absorption peaks at 1740cm^{-1} and 1240cm^{-1}, which are carbonyl (-C = O) and C-O stretching vibrations, respectively. The reason is that the three-dimensional network structure of XLPE is destroyed by the strong force of the S^3M equipment, and a large number of free radicals are generated, which further react with oxygen in the air and introduce oxygen-containing groups[26]. As shown in Figure. 2(b), the composition of asphalt is very complex. The FTIR of asphalt shows strong absorption vibration peaks at 650 ~ 1700cm^{-1} and 2700 ~ 3000cm^{-1}, and the absorption peak at 3430cm^{-1} is produced by the associated hydroxyl groups in water molecules. Asphalt is a mixture of saturated aromatic hydrocarbons and compounds, alkyl hydrocarbons, and heteroatom derivatives such as oxygen and sulfur[27]. Therefore, the internal molecular structure and functional groups are very complicated. As shown in Figure.2(b), the asphalt-modified WP-XLPE composite material has no new absorption peak, indicating that there is no obvious chemical reaction between the two components, and the modification mechanism is mainly physical.

X-ray photoelectron spectroscopy can obtain chemical bond composition information in the range of 2-10nm on the surface of the material. From the XPS spectrum of the WP-XLPE cable before and after milling in the figure.3, the results consistent with FTIR can be obtained. In the high-resolution spectra of C and O, it can be seen that the powder after milling has a new peak at the position corresponding to the carbonyl group[28], indicating that when the powder is decomposed by force, there is indeed a process of reacting with oxygen to form a C = O bond. This is a part of the methylene groups deformed and broken under the action of considerable mechanical stresses by S^3M technology, and oxidized into new carbonyl groups[29, 30]. However, the EVA in the cable brings natural hydroxyl groups to the WP-XLPE powder, which can also be seen in the results[31]. This shows that the S^3D equipment developed by our research group is not simply a grinding process but a solid-phase mechanochemical reactor. In this process, the thermosetting cross-linked molecular structure is destroyed, and the chemical bonds are partially reorganized.

Figure.3 also shows the C and O high-resolution spectra of asphalt modified WP-XLPE composites with different contents. Compared with the pure WP-XLPE without asphalt, the content of the C = O bond has increased from 39.8–51%, which indicates that the free radicals generated during the milling process are continuously oxidized to produce carbonyl groups during the thermoplastic processing. Since there was no chemical bond breaking or formation during the asphalt modification process, no new peaks appeared in the XPS results. Asphalt plays a role as a plasticizer that weakens intermolecular forces and increases free volume in composite materials. This is also mutually corroborated by the absence of new absorption peaks in the FTIR spectrum.

3.2 Compatibility of Asphalt and WP-XLPE

The dynamic mechanical properties are shown in Figure.4. The result of DMA reflects the good compatibility of asphalt and WP-XLPE. The α and β transition peaks of different asphalt content are in the same temperature range, indicating that the compatibility between the two phases is good; in other words, the addition of asphalt does not affect the tan δ of WP-XLPE. The transition area of adding asphalt becomes narrower, which also shows that the distribution between the two phases is uniform[32]. The increase in peak intensity, mainly contributed by the amorphous phase, is due to the easier movement of small molecules in the asphalt component, which makes the segment movement more frictional[33]. The movement of the relaxation temperature to high temperature indicates that the amorphous WP-XLPE is arranged more regularly under the action of asphalt, and the structure density is improved, which makes up for the disordered structure caused by the solid phase mechanochemistry.

The storage modulus reflects the rigidity of the material. As shown in the figure.4(b), the content of asphalt has a significant effect on it. When the temperature is below zero, the chain segment is frozen and yet to move, but the lower molecular weight asphalt can better transfer the force received to the rigid particles, thereby increasing the storage modulus of the material. In addition, as the temperature increases, the matrix begins to soften, and with relaxation, the storage modulus decreases. Contrary to the elastic modulus, the loss modulus is a measure of the energy loss when the composite material is deformed to reflect the toughness of the material. The loss modulus peak around − 25℃ in the figure.4(c) indicates that the asphalt makes the amorphous part of WP-XLPE more regular and hinders the movement of the chain segment. There is a rule that the higher the content, the more obvious the restriction

3.3 Distribution of Asphalt and WP-XLPE

To carefully observe the phase morphology of the two-phase distribution, the cross-section of the composite material was analyzed by SEM. As shown in Figure.5, the section of the pure XLPE without asphalt is not only randomly scattered with particles, but also has many scaly protrusions; on the contrary, the section of the composite with asphalt is very flat, with no trace of filler at all. It can be concluded that the two-phase dispersion is very uniform, and there is no phase separation or incompatibility. Actually, WP-XLPE cable is a complex mixture, in which the inorganic filler hinders the flow of the melt during the melting process. The section without asphalt can find that the distribution of these fillers is very uneven, which affects the performance of the material. The addition of asphalt wraps these fillers and makes the fillers more smoothly distributed in the matrix. Even in the cross-section, its existence cannot be seen, showing a very smooth shape.

Observing the etched section in Figure.6, you can see the circular or deep groove-like voids left by the asphalt after being etched, which shows that the asphalt has a dispersed state and a continuous state. The distribution between asphalt and WP-XLPE has both a typical island-like structure surrounded by asphalt and a sheet-like structure after melting, indicating that the 3D network structure is destroyed under the action of solid-state mechanochemistry[34].

Under the effect of S3M technology, WP-XLPE is divided into two parts: fusible polyethylene and non-melting cross-linked network. It brings about two different behaviors under interaction with asphalt: the movable part of the chain formed under shear is melted and mixed with asphalt to form an interlocking continuous layered structure; the infusible part is wrapped in asphalt to form an island structure. The asphalt here is like a plasticizer, connecting the three parts of amorphous, crystalline, and cross-linked. It makes the movement of the molecular chain more smoothly at high temperatures and more regularly during thermoplastic processing. In addition, the sea-island structure provides toughness to the material.

3.4 Thermal Performance

As shown in Figure.7(a, b), with the addition of asphalt, the processing temperature of the material is significantly reduced. There is also a trend that the more the amount added, the more obvious the melting temperature and crystallinity will decrease. The content of asphalt destroys the crystal lattice arrangement of PE and affects the crystallization process of its material, causing the formation of imperfect crystal, resulting in a decrease in melting temperature and crystallinity[35]. During the cooling crystallization process, the endothermic peak shifts to low temperature with the addition of asphalt. The reason is that the volume of molecular chain movement increases, so that crystallization can be achieved at lower temperatures[36]. In addition, this also reflects that the addition of asphalt does act as a plasticizer, which makes the molecular chain move easily and contributes to good thermoplastic processing performance.

As far as the thermal stability in Figure.7(c) is concerned, the thermal weight loss of materials mainly includes two stages: the first stage is 250–400℃, which is mainly the thermal degradation of EVA and asphalt; the second stage is 400–500℃, which is mainly the thermal degradation of the WP-XLPE matrix. Obviously, the whole process is mainly based on the second stage. In the first stage, because asphalt is a low-molecular mixture with an average molecular weight of about 1,000, as the temperature rises, the asphalt in the composite material begins to decompose first. The low-temperature decomposition temperature is relatively stable, but the mass lost at this temperature increases with the increase of the asphalt content. In the second stage, the decomposition temperature tends to move to high temperature with the addition of asphalt, indicating that the thermal stability of the composite material has become better[37].

3.5 Processing Performance

In this paper, a high-pressure capillary rheometer was used to test the processing performance of composite materials with different asphalt additions. It can be seen from Figure.8(a) that this is a typical shear thinning situation, and as the asphalt content increases, the shear viscosity of the material decreases, especially in the low-frequency range[38]. The same result can also be obtained in the torque rheology curve in Figure.8(b). When the asphalt addition amount is 20%, the torque drops suddenly, indicating the melt viscosity is low and the thermoplastic processing is easier. This shows that when the material is in the molten state, asphalt as a plasticizer moves between the cross-linked phase and the amorphous phase[39]. At the same time, it plays a role in reducing the entanglement and friction between

the molten phase and the infused phase to make the melt flow smoothly. The plasticization mechanism is called the volume effect, because of the addition of asphalt increasing the distance between polymer molecules and decreasing the force between the molecules[40, 41]. The weakening of van der Waals force brings about a drop in melt viscosity. The existence of asphalt makes up for the shortcomings of difficult thermoplastic processing of pure WP-XLPE powder.

3.6 Mechanical Performance

The tensile data of pure WP-XLPE in the figure.9 shows that after ten times of milling, the waste cable material has regained the thermoplastic processability and the recycled material also has better mechanical performance. This is consistent with the statement in a large number of documents: S^3M technology has the function of de-crosslinking and provides ideas for recycling thermoset plastics. For asphalt-modified WP-XLPE composite materials, the addition of asphalt not only improves the processing performance of WP-XLPE but also affects the mechanical properties of the material. As the asphalt content increases, Young's modulus and tensile strength decrease to a certain extent, but the fracture energy and elongation at break have a peak. When the asphalt content is 10%, the elongation can reach 322%, and the tensile strength remains above 10MPa.The reason for the above phenomenon are as follows: asphalt has the effect of weakening the intermolecular force of WP-XLPE, increasing the fluidity of the molecular chain, and reducing the crystallinity of the molecular chain, which leads to a decrease in strength and an increase in toughness. This is no different from ordinary plasticizers, but the similar chemical composition and structure lead to good compatibility with the fusible phase. Finally, it can be directly processed by screw extrusion to obtain a sheet with a stable structure and smooth surface as shown in Figure.9(c).

4. Conclusion

Although the powder processed by S^3M technology can be processed by thermoplastic, the filler and cross-linked part in the material hinder the movement of the molecular chain, which makes the screw extrusion molding difficult and the sample surface rough. The purpose of this research is to improve the melt fluidity of WP-XLPE. The addition of asphalt can solve the dispersion relationship among filler, cross-linked part, and decross-linked part. Due to the principle of like dissolves like, the two have good compatibility. Furthermore, the role of asphalt is also highlighted: increasing the intermolecular gap, promoting molecular movement, and reducing melt viscosity, which effectively reduced the difficulty of thermoplastic processing. The asphalt with good fluidity also entrains the filler in WP-XLPE to make it more evenly dispersed in the matrix. In addition, the asphalt and the non-melting cross-linked part form a sea-island structure, which enhances the toughness of the material to a certain extent. When the asphalt content is 10%, the elongation can reach 322%, and the tensile strength remains above 10MPa. Different from the complex process of traditional waterproofing membranes, this material can be directly prepared into continuous membranes by screw extrusion. At last, the use of WP-XLPE cable material as the matrix also provides a new direction for large-scale recycling of waste, bringing considerable economic and social benefits.

Declarations

Acknowledgment

This work is financed by the National Key Research and Development Program of China (2019YFC1908200), the National Natural Science Foundation of China (51861165203), and the Program for Featured Directions of Engineering Multidisciplines of Sichuan University (No: 2020SCUNG203).

Declarations

Funding: This work is supported by the National Key Research and Development Program of China (2019YFC1908200), the National Natural Science Foundation of China (51861165203), and the Program for Featured Directions of Engineering Multidisciplines of Sichuan University (No: 2020SCUNG203).

Conflicts of interest/Competing interests:

The authors declared no conflict of interest.

Availability of data and material:

The data are available from the corresponding author on reasonable request.

Code availability:

Not applicable

Authors' contributions:

All authors contributed to the study conception and design. Material preparation, data collection and analysis were performed by Yi Liao. And all authors commented on previous versions of the manuscript. All authors read and approved the final manuscript.

Ethics approval: This research was not involved with any human or animal experiment. And ethics approval was not required for this research.

Consent to participate:

All authors agree to submit.

Consent for publication:

All authors agree to publish.

References

1. Kato, T., Onozawa, R., Miyake, H., Tanaka, Y., Takada, T. (2017) Properties of Space Charge Distributions and Conduction Current in XLPE and LDPE under DC High Electric Field.Electr Eng Jpn 198 19-26. http://dx.doi.org/10.1002/eej.22926.
2. Chang, B.P., Akil, H.M., Nasir, R.B.M., Bandara, I.M.C.C.D., Rajapakse, S. (2014) The effect of ZnO nanoparticles on the mechanical, tribological and antibacterial properties of ultra-high molecular weight polyethylene.J Reinf Plast Comp 33 674-686. http://dx.doi.org/10.1177/0731684413509426.
3. Tone, S., Hasegawa, M., Pezzotti, G., Puppulin, L., Sudo, A. (2017) Effect of e-beam sterilization on the in vivo performance of conventional UHMWPE tibial plates for total knee arthroplasty.Acta Biomater 55 455-465. http://dx.doi.org/10.1016/j.actbio.2017.03.040.
4. Al-Malaika, S., Riasat, S., Lewucha, C. (2017) Reactive antioxidants for peroxide crosslinked polyethylene.Polym Degrad Stabil 145 11-24. http://dx.doi.org/10.1016/j.polymdegradstab.2017.04.013.
5. Niu, Y.H., Liang, W.B., Zhang, Y.L., Chen, X.L., Lai, S.Y., Li, G.X., Wang, D.J. (2016) Crosslinking kinetics of polyethylene with small amount of peroxide and its influence on the subsequent crystallization behaviors.Chinese J Polym Sci 34 1117-1128. http://dx.doi.org/10.1007/s10118-016-1819-z.
6. Wang, H.L., Xu, L., Li, R., Hu, J.T., Wang, M.H., Wu, G.Z. (2016) Improving the creep resistance and tensile property of UHMWPE sheet by radiation cross-linking and annealing.Radiat Phys Chem 125 41-49. http://dx.doi.org/10.1016/j.radphyschem.2016.03.009.
7. Häußler, M., Eck, M., Rothauer, D., Mecking, S. (2021) Closed-loop recycling of polyethylene-like materials.Nature 590 423-427. http://dx.doi.org/10.1038/s41586-020-03149-9.
8. Singh, N., Hui, D., Singh, R., Ahuja, I.P.S., Feo, L., Fraternali, F. (2017) Recycling of plastic solid waste: A state of art review and future applications.Composites Part B: Engineering 115 409-422. http://dx.doi.org/10.1016/j.compositesb.2016.09.013.
9. Han, S., Bang, J., Choi, D.H., Hwang, J., Kim, T., Oh, Y., Hwang, Y., Choi, J., Hong, J. (2020) Surface Pattern Analysis of Microplastics and Their Impact on Human-Derived Cells.Acs Applied Polymer Materials 2 4541-4550. http://dx.doi.org/10.1021/acsapm.0c00645.
10. Goto, T., Ashihara, S., Yamazaki, T., Okajima, I., Sako, T., Iwamoto, Y., Ishibashi, M., Sugeta, T. (2011) Continuous Process for Recycling Silane Cross-Linked Polyethylene Using Supercritical Alcohol and Extruders.Ind Eng Chem Res 50 5661-5666. http://dx.doi.org/10.1021/ie101772x.
11. Feng, X., Li, Q., Wang, K. (2021) Waste Plastic Triboelectric Nanogenerators Using Recycled Plastic Bags for Power Generation.Acs Appl Mater Inter 13 400-410.

http://dx.doi.org/10.1021/acsami.0c16489.

12. Faraj, R.H., Ali, H.F.H., Sherwani, A.F.H., Hassan, B.R., Karim, H. (2020) Use of recycled plastic in self-compacting concrete: A comprehensive review on fresh and mechanical properties.J Build Eng 30. http://dx.doi.org/ARTN 101283

10.1016/j.jobe.2020.101283.

13. Backstrorn, E., Odelius, K., Hakkarainen, M. (2019) Designed from Recycled: Turning Polyethylene Waste to Covalently Attached Polylactide Plasticizers.Acs Sustain Chem Eng 7 11004-11013. http://dx.doi.org/10.1021/acssuschemeng.9b02092.
14. Al-Salem, S.M., Antelava, A., Constantinou, A., Manos, G., Dutta, A. (2017) A review on thermal and catalytic pyrolysis of plastic solid waste (PSW).Journal of Environmental Management 197 177-198. http://dx.doi.org/10.1016/j.jenvman.2017.03.084.
15. Zhang, X., Lei, H., Chen, S., Wu, J. (2016) Catalytic co-pyrolysis of lignocellulosic biomass with polymers: a critical review.Green Chemistry 18 4145-4169. http://dx.doi.org/10.1039/c6gc00911e.
16. Kumagai, S., Yoshioka, T. (2016) Feedstock Recycling via Waste Plastic Pyrolysis.Journal of the Japan Petroleum Institute 59 243-253. http://dx.doi.org/10.1627/jpi.59.243.
17. Yang, S.Q., Bai, S.B., Wang, Q. (2015) Preparation of fine fiberglass-resin powders from waste printed circuit boards by different milling methods for reinforcing polypropylene composites.Journal of Applied Polymer Science 132. http://dx.doi.org/ARTN 42494

10.1002/app.42494.

18. Yang, S.Q., Wei, B.J., Wang, Q. (2020) Superior dispersion led excellent performance of wood-plastic composites via solid-state shear milling process.Compos Part B-Eng 200. http://dx.doi.org/ARTN 108347

10.1016/j.compositesb.2020.108347.

19. He, P., Bai, S.B., Wang, Q. (2016) Structure and performance of Poly(vinyl alcohol)/wood powder composite prepared by thermal processing and solid state shear milling technology.Compos Part B-Eng 99 373-380. http://dx.doi.org/10.1016/j.compositesb.2016.06.006.
20. Yang, S.Q., Bai, S.B., Wang, Q. (2016) Morphology, mechanical and thermal oxidative aging properties of HDPE composites reinforced by nonmetals recycled from waste printed circuit boards.Waste Manage 57 168-175. http://dx.doi.org/10.1016/j.wasman.2015.11.005.
21. Sun, F.S., Yang, S.Q., Wang, Q. (2020) Selective Decomposition Process and Mechanism of Si-O-Si Cross-Linking Bonds in Silane Cross-Linked Polyethylene by Solid-State Shear Milling.Ind Eng Chem Res 59. http://dx.doi.org/10.1021/acs.iecr.0c01956.
22. Li, D.D., Greenfield, M.L. (2014) Chemical compositions of improved model asphalt systems for molecular simulations.Fuel 115 347-356. http://dx.doi.org/10.1016/j.fuel.2013.07.012.

23. Gawel, I., Stepkowski, R., Czechowski, F. (2006) Molecular interactions between rubber and asphalt.Ind Eng Chem Res 45 3044-3049. http://dx.doi.org/10.1021/ie050905r.
24. Zhao, B.W., Qi, L.J., Zhao, Q.Q., Zhu, X.X. (2017) Optimization and Practice of Energy-saving and Emission-reduction System for Production Process of Modified Asphalt Waterproofing Membrane.Procedia Engineer 205 930-936. http://dx.doi.org/10.1016/j.proeng.2017.10.131.
25. Italia, P. (1996) Polypropylene-asphalt mixtures for waterproofing membranes.Abstr Pap Am Chem S 212 72-Fuel.
26. Wu, H.J., Liang, M., Lu, C.H. (2012) Non-isothermal crystallization kinetics of peroxide-crosslinked polyethylene: Effect of solid state mechanochemical milling.Thermochim Acta 545 148-156. http://dx.doi.org/10.1016/j.tca.2012.07.008.
27. Jemison, H.B., Burr, B.L., Davison, R.R., Bullin, J.A., Glover, C.J. (1990) Application and Use of the Atr, Ft-Ir Method to Asphalt Aging Studies.Abstr Pap Am Chem S 200 45-Petr.
28. Silverstein, R.M., Rodin, J.O. (1965) SPECTROMETRIC IDENTIFICATION OF ORGANIC COMPOUNDS ON A MILLIGRAM SCALE - USE OF COMPLEMENTARY INFORMATION.Microchemical Journal 9 301-+. http://dx.doi.org/10.1016/0026-265x(65)90049-4.
29. Bagus, P.S., Ilton, E.S., Nelin, C.J. (2013) The interpretation of XPS spectra: Insights into materials properties.Surf Sci Rep 68 273-304. http://dx.doi.org/10.1016/j.surfrep.2013.03.001.
30. Wu, H.J., Liang, M., Lu, C.H. (2011) Morphological and Structural Development of Recycled Crosslinked Polyethylene During Solid-State Mechanochemical Milling.Journal of Applied Polymer Science 122 257-264.
31. Xu, T., Huang, X.M. (2010) Study on combustion mechanism of asphalt binder by using TG-FTIR technique.Fuel 89 2185-2190. http://dx.doi.org/10.1016/j.fuel.2010.01.012.
32. Shieh, Y.T., Chuang, H.C. (2001) DSC and DMA studies on silane-grafted and water-crosslinked LDPE/LLDPE blends.Journal of Applied Polymer Science 81 1808-1816. http://dx.doi.org/10.1002/app.1614.abs.
33. Chambers, R.C., Jones, W.E., Haruvy, Y., Webber, S.E., Fox, M.A. (1993) INFLUENCE OF STERIC EFFECTS ON THE KINETICS OF ETHYLTRIMETHOXYSILANE HYDROLYSIS IN A FAST SOL-GEL SYSTEM.Chemistry of Materials 5 1481-1486. http://dx.doi.org/10.1021/cm00034a018.
34. Vollmer, I., Jenks, M.J.F., Roelands, M.C.P., White, R.J., van Harmelen, T., de Wild, P., van Der Laan, G.P., Meirer, F., Keurentjes, J.T.F., Weckhuysen, B.M. (2020) Beyond Mechanical Recycling: Giving New Life to Plastic Waste.Angewandte Chemie-International Edition 59 15402-15423. http://dx.doi.org/10.1002/anie.201915651.
35. Rahman, M., Brazel, C.S. (2004) The plasticizer market: an assessment of traditional plasticizers and research trends to meet new challenges.Progress in Polymer Science 29 1223-1248. http://dx.doi.org/10.1016/j.progpolymsci.2004.10.001.
36. Vaughan, A.S., Swingler, S.G. (1993) Thermal-Analysis of Polymeric Sheathing Materials for Fiber Optic Communication Cables.Iee Conf Publ 363 57-60.

37. Zuo, M., Zheng, Q. (2008) Correlation between rheological behavior and structure of multi-component polymer systems.Science in China Series B-Chemistry 51 1-12. http://dx.doi.org/10.1007/s11426-008-0022-7.
38. Arrigo, R., Malucelli, G. (2020) Rheological Behavior of Polymer/Carbon Nanotube Composites: An Overview.Materials 13. http://dx.doi.org/10.3390/ma13122771.
39. Yn-hwang, L., 2011. Molecular theory of polymer viscoelasticity - nonlinear relaxation modulus of entangled polymers.
40. Yu, W., Wu, Z.G., Zhou, C.X., Zhao, D.L. (2003) Linear viscoelasticity calculation of exfoliated polymer/layer silicate nanocomposites.Chemical Journal of Chinese Universities-Chinese 24 715-718.
41. Kubo, K., Masamoto, J. (2002) Application of elastomer-toughened poly(phenylene sulfide) to gasohol material.Kobunshi Ronbunshu 59 88-92. http://dx.doi.org/DOI 10.1295/koron.59.88.

Figures

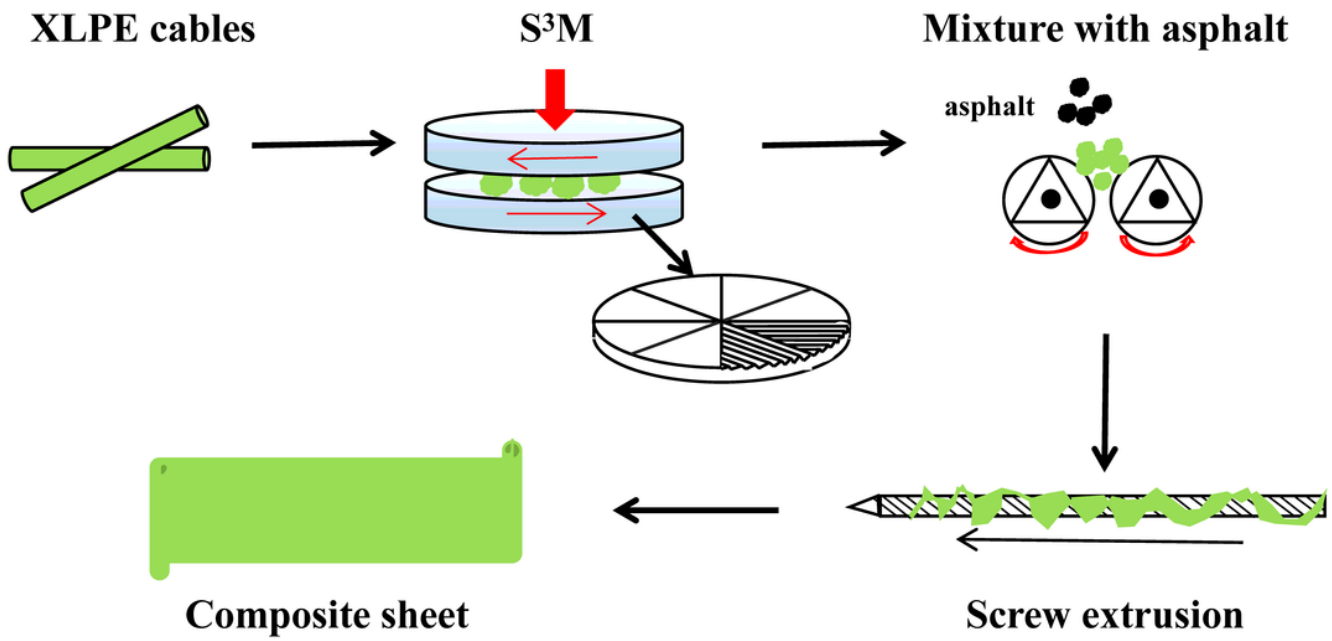

Figure 1

Scheme of recycling WP-XLPE and preparing composite sheet

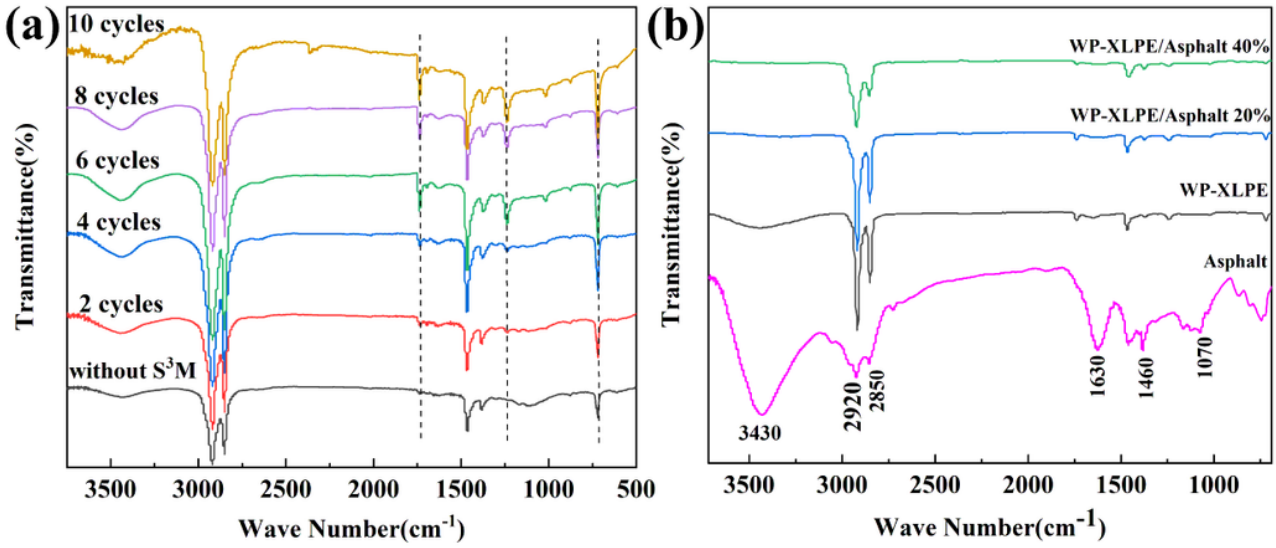

Figure 2

FTIR spectra of WP-XLPE with different milling cycles (a), asphalt, and the composite (b)

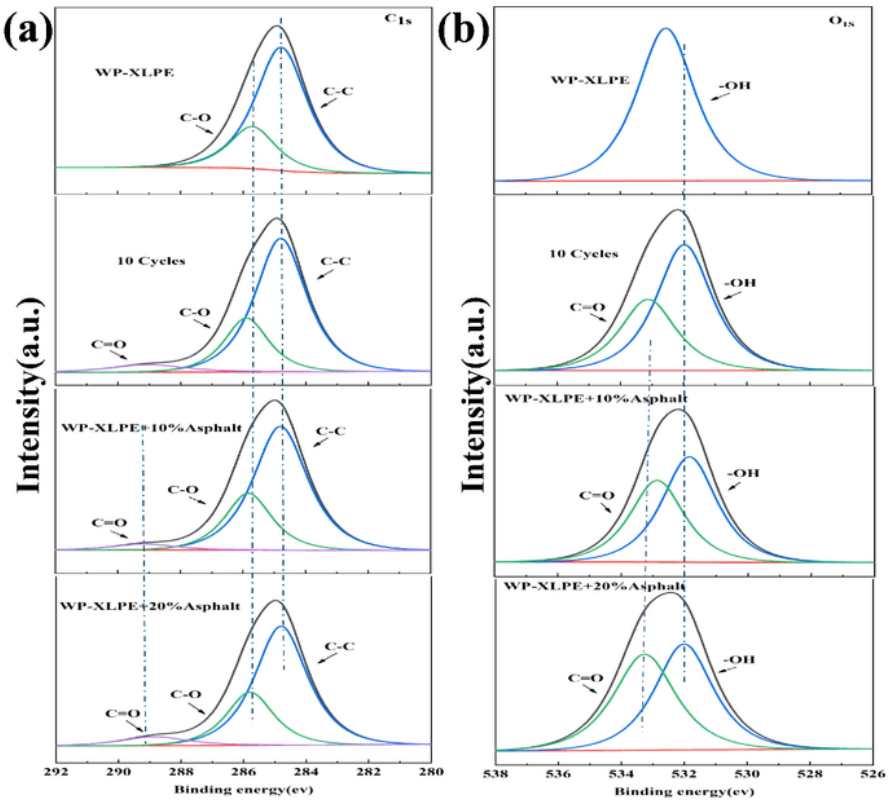

Figure 3

Comparison of XPS spectra of WP-XLPE before and after S3M, and the composite with different asphalt content: XPS spectra for C1s (a), O1s(b)

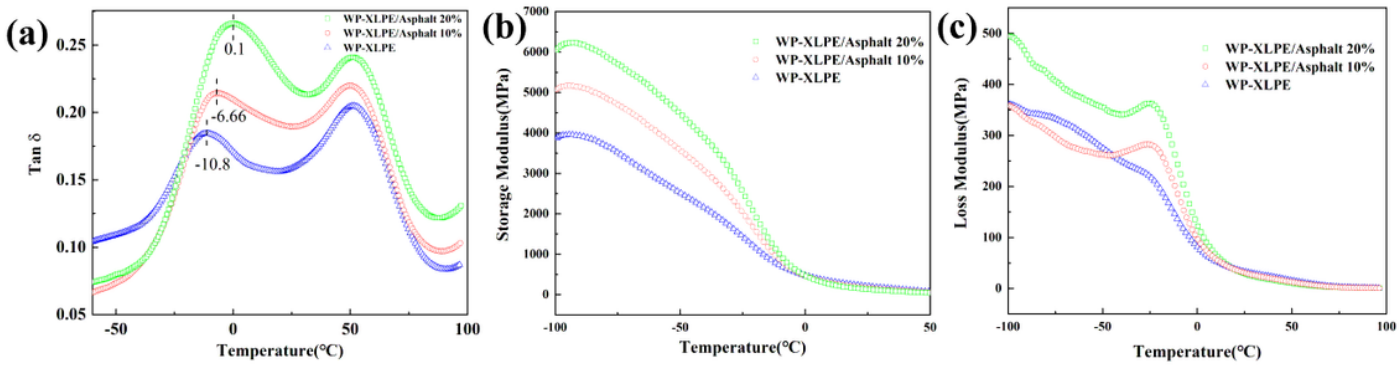

Figure 4

DMA curves of WP-XLPE/asphalt composites with different asphalt content

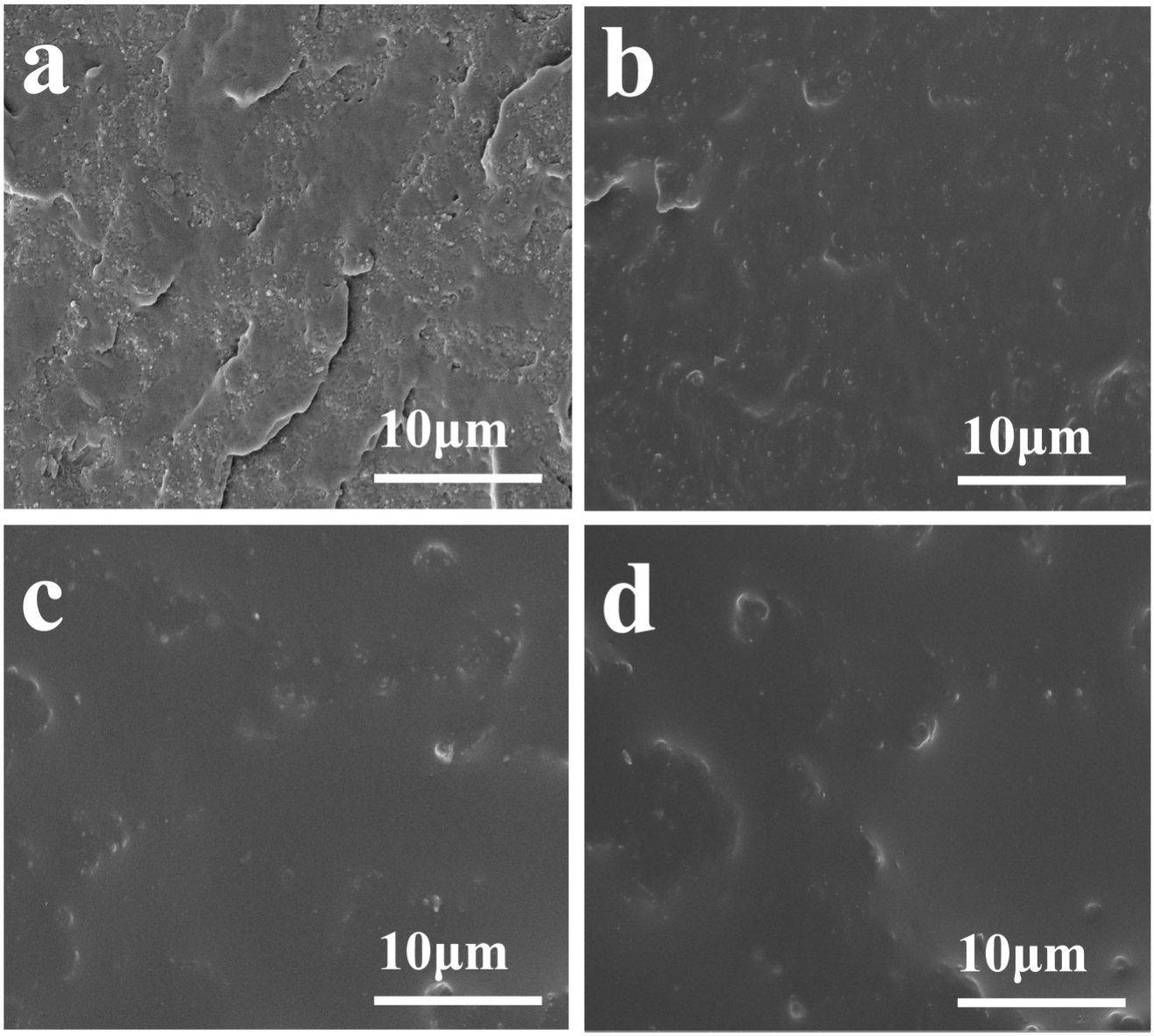

Figure 5

SEM images of the fracture surface of WP-XLPE/asphalt composites: without asphalt (a),10wt% asphalt (b),20wt% asphalt (c),30wt% asphalt (d)

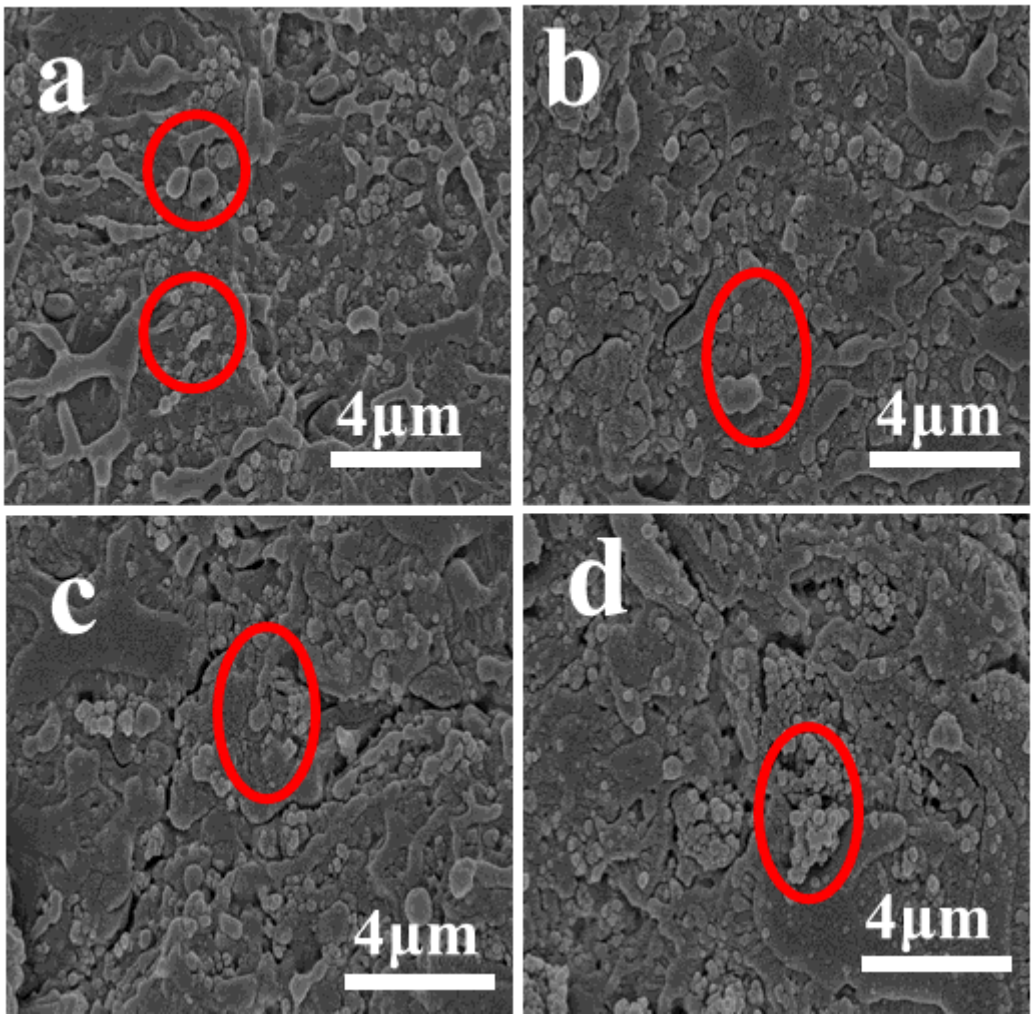

Figure 6

SEM images of the fracture surface after etched of WP-XLPE/asphalt composites:10wt% asphalt (a),20wt% asphalt (b),30wt% asphalt (c),40wt% asphalt (d)

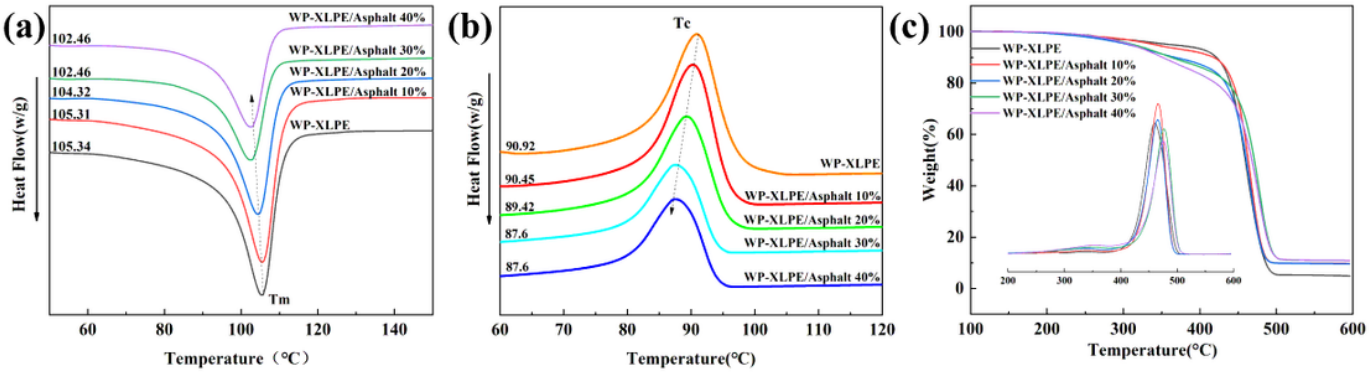

Figure 7

The DSC curve (a, b) and TGA curve (c) of composites with different asphalt content

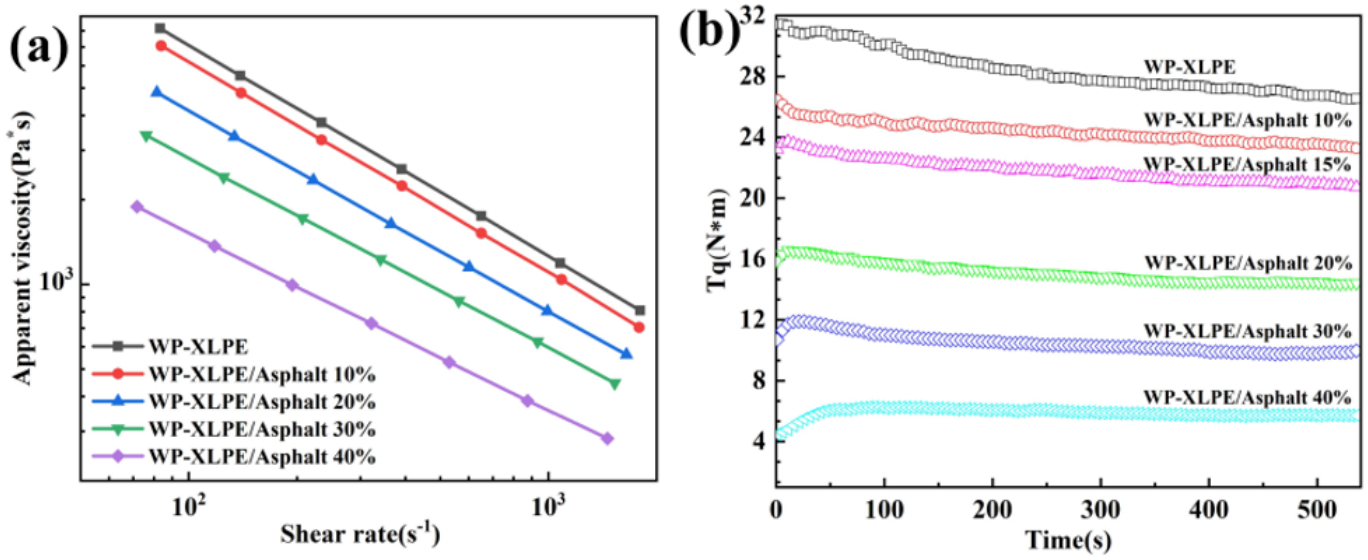

Figure 8

Capillary rheological curve (a) and the torque variation (b) of composites with different asphalt content

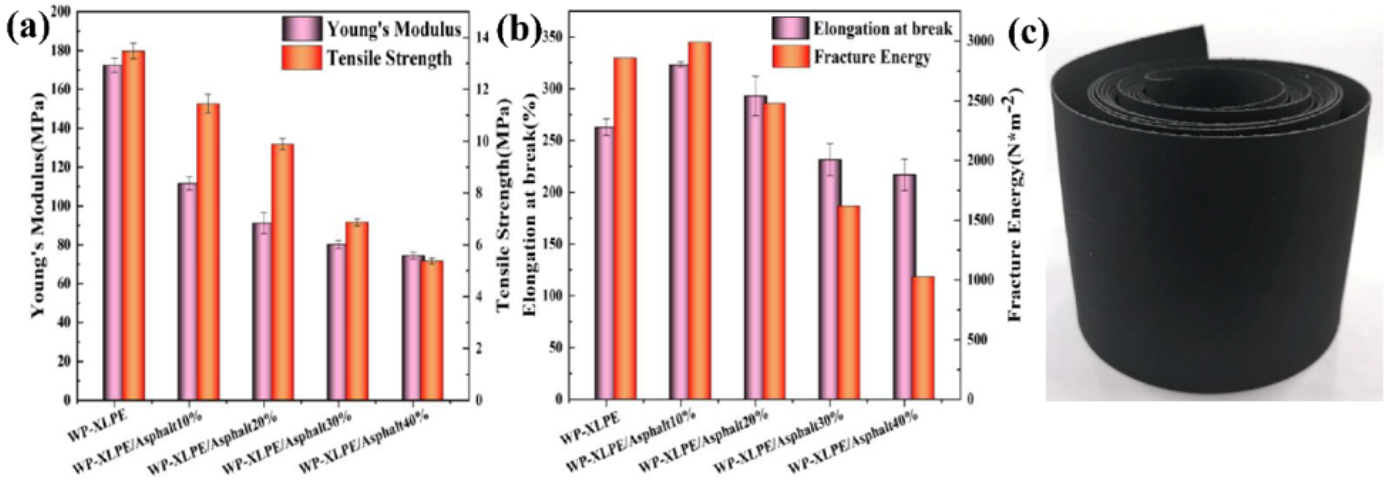

Figure 9

Tensile performance of composites with different asphalt content (a, b); digital photographs of WP-XLPE/asphalt extruded sheet blends(c)